Ecotoxicology and Environmental Safety 252 (2023) 114587

Contents lists available at ScienceDirect

Ecotoxicology and Environmental Safety

journal homepage: www.elsevier.com/locate/ecoenv

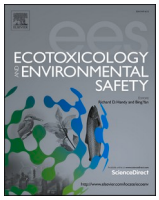

Efficient bioconversion of lignocellulosic waste by a novel computationally screened hyperthermostable enzyme from a specialized microbiota

Shohreh Ariaeenejad [a,*], Kaveh Kavousi [b], Behrouz Zolfaghari [c,g], Swapnoneel Roy [d], Takeshi Koshiba [e], Ghasem Hosseini Salekdeh [a,f]

[a] Department of Systems and Synthetic Biology, Agricultural Biotechnology Research Institute of Iran (ABRII), Agricultural Research Education and Extension Organization (AREEO), Karaj, Iran
[b] Laboratory of Complex Biological Systems and Bioinformatics (CBB), Department of Bioinformatics, Institute of Biochemistry and Biophysics (IBB), University of Tehran, Tehran, Iran
[c] CSE Department, Indian Institute of Technology (IIT) Guwahati, Guwahati, Assam, India
[d] School of Computing, University of North Florida, Jacksonville, FL, USA
[e] Department of Mathematics, Faculty of Education and Integrated Arts and Sciences, Waseda University, Japan
[f] Department of Molecular Sciences, Macquarie University, Sydney, 2109 NSW, Australia
[g] Department of Computer Engineering, Faculty of Engineering, Haliç University Eyüpsultan, Istanbul

ARTICLE INFO

Edited by: Dr G Liu

Keywords:
Hyperthermostable
Xylanase
Metagenome
Lignocellulosic recalcitrant

ABSTRACT

A large amount of lignocellulosic waste is generated every day in the world, and their accumulation in the agroecosystems, integration in soil compositions, or incineration for energy production has severe environmental pollution effects. Using enzymes as biocatalysts for the biodegradation of lignocellulosic materials, especially in harsh processing conditions, is a practical step towards green energy and environmental biosafety. Hence, the current study focuses on enzyme computationally screened from camel rumen metagenomics data as specialized microbiota that have the capacity to degrade lignocellulosic-rich and recalcitrant materials. The novel hyperthermostable xylanase named PersiXyn10 with the performance at extreme conditions was proper activity within a broad temperature (30–100 ℃) and pH range (4.0–11.0) but showed the maximum xylanolytic activity in severe alkaline and temperature conditions, pH 8.0 and temperature 90 ℃. Also, the enzyme had highly resistant to metals, surfactants, and organic solvents in optimal conditions. The introduced xylanase had unique properties in terms of thermal stability by maintaining over 82% of its activity after 15 days of incubation at 90 ℃. Considering the crucial role of hyperthermostable xylanases in the paper industry, the PersiXyn10 was subjected to biodegradation of paper pulp. The proper performance of hyperthermostable PersiXyn10 on the paper pulp was confirmed by structural analysis (SEM and FTIR) and produced 31.64 g/L of reducing sugar after 144 h hydrolysis. These results proved the applicability of the hyperthermostable xylanase in biobleaching and saccharification of lignocellulosic biomass for declining the environmental hazards.

1. Introduction

Nowadays, the world is facing the problem of different environmental pollution and declining eco-pollution is the primary demand of today's world (Tsang et al., 2019). Tremendous amounts of agro-based industries, such as pulp and paper mills, are produced every

Abbreviation: SEM, Scanning electron microscope; FTIR, Fourier transform infrared spectroscopy; DTT, Dithiothreitol; EDTA, Ethylenediaminetetra acetic acid; SDS, Sodium dodecyl sulfate; PMSF, Phenylmethylsulfonyl fluoride; CTAB, Cetrimonium bromide; DMSO, Dimethyl sulfoxide; DNS, 3,5-Dinitrosalicylic acid; BSA, Bovine serum albumin; TAXyl, Thermal activity prediction for Xylanase; NCBI, National Center for Biotechnology Information; CDD, Conserved Domains Database; PCR, Polymerase chain reaction; LB, Lysogeny broth; IPTG, Isopropyl β-D-1-thiogalactopyranoside; SDS-PAGE, Sodium dodecyl sulfate-polyacrylamide gel electrophoresis; NTA, Nitrilotriacetic acid; CD, Circular dichroism; UV, Ultraviolet; PSSM, Position-specific scoring matrix; PDB, Protein Data Bank; E-value, Expect value. pLDDT, per residue Local Distance Difference Test; PAE, Predicted Aligned Error.

* Correspondence to: Department of Systems and Synthetic Biology, Agricultural Biotechnology Research Institute of Iran (ABRII), P. O. Box: 31535–1897, 2704539 Karaj, Iran.
E-mail addresses: shariaee@gmail.com, sh.ariaee@abrii.ac.ir (S. Ariaeenejad).

https://doi.org/10.1016/j.ecoenv.2023.114587
Received 23 June 2022; Received in revised form 24 January 2023; Accepted 28 January 2023
Available online 7 February 2023

day, and most of these wastes contain lignocellulosic compounds. That can be utilized to generate value-added products such as fuel and energy while reducing the volume of waste (Bilal et al., 2019). However, the major drawback in the utilization of biomass in industrial applications is its recalcitrant structure which contains plenty of monosaccharides, such as xylose (Tyagi and Sharma, 2021). Bioremediation is a biological mechanism of recycling wastes into another form that can be used and reused by other organisms. Bioremediation by natural enzymes in microorganisms or plants as biocatalysts reduces the activation energy and leads to rapid and complete degradation of lignocellulosic substrates.

Hemicellulose is the second most abundant polysaccharide in the lignocellulosic biomass, representing approximately 30% of lignocellulosic materials (Kim et al., 2018). Xylanases are responsible for converting the complex matrix of hemicellulose into fermentable products by cleaving the β-1,4 xylan backbone to create xylooligosaccharides and xylose (Collins et al., 2005). This group of enzymes has versatile commercial utility, including pulp biobleaching in the production of paper, animal feed, pharmaceuticals, clarifying agents in juices and wines, and waste treatment (Nigam, 2013). These enzymes are crucial in the biorefining of lignocellulosic biomass and can enhance the access of cellulase to the cellulose surface by hydrolysis of xylan (You et al., 2018). Some profound characteristics, including high specific activity, thermal stability, and resistance to cations and inhibitors, are vital for xylanase applications (Yeoman et al., 2010). Particularly, the lack of xylanases thermostability is a bottleneck for such applications. The thermal stability of xylanases is associated with countless advantages in industrial processes, such as stability against denaturing conditions and improved hydrolysis performance (Yeoman et al., 2010). Alkaline, thermostable xylanases find application in the bioconversion process and pulp bleaching industry which produces 17% of the total global waste (Haile et al., 2021). In addition, xylanases with high thermal stability are utilized in the brewing and feed industry for pelleting process and longer hydrolysis at high temperatures (Wang et al., 2016). Despite investigating multiple xylanases with activity and stability under high temperatures, they cannot meet industrial demands regarding their inactivation under extreme temperatures. Several techniques have been developed to produce robust, thermostable xylanases to meet industrial demands. Hyperthermophile microorganisms are the sources for the production of hyperthermostable enzymes. These xylanases are beneficial for industrial usage regarding the high enzyme accessibility to the lignocellulose cell wall at high temperatures (Atomi et al., 2011).

The need for white biotechnology to produce new enzymes from uncultivated microbial species and their practical use for modern industrial society's sustainable economic future development is strongly seen. Acknowledging that the cultivation of most microorganisms is not possible using conventional methods, metagenomics offers a suitable solution for studying the whole microbial community and related enzymes that are directly isolated from an environment (Ahmad et al., 2019). The camel diet is dominated by a wide range of low-quality woody plants and various halophytes, aromatic plant species, and tree biomass, while many other ruminants do not use this feed source (Gharechahi et al., 2015; Samsudin et al., 2012). As a result, the camel rumen microbial community must have the capacity to break down such lignocellulosic-rich substances. Given that the fiber compositions influence the composition of ruminal bacterial species and consequently the diversity of enzymes in the feed, the camel rumen can potentially be considered a source for novel effective enzymes. This approach identifies structurally novel enzymes with stability towards a specific parameter such as temperature, pH, or solvents. Various robust enzymes have been discovered through the metagenomic approach for a vast number of industrial applications and the reduction of environment effluents (Ariaeenejad et al., 2022; S. Shohreh Ariaeenejad et al., 2020; S. Ariaeenejad et al., 2020; Motamedi et al., 2021). The thermostable xylanases have been identified from various metagenomic sources to degrade xylan efficiently (Shohreh Ariaeenejad et al., 2019; S. Ariaeenejad et al., 2019; Joshi et al., 2020). Due to the great need to screen novel stable xylanases in harsh conditions, especially high temperatures, the computational screening method is suitable without high laboratory costs in basic research and industrial applications(Ariaeenejad et al., 2021).

In this study, PersiXyn10 was identified and produced in the laboratory using an *in-silico* screening strategy and computational methods. The optimal activity and temperature stability (30–100 ℃) and pH (4.0–11.0) of the enzyme were determined. Preservation of the structure and activity of the enzyme against metal ions, inhibitors, and various solvents was measured after one month of storage at 90 ℃. As far as the environmental effects of the thermostable alkaline xylanases are concerned, the PersiXyn10 investigated the potential biobleaching of the waste paper pulp in agro-based industries.

2. Materials and methods

2.1. Chemical and reagents

The birchwood xylan, metal ions, ethanol, methanol, dithiothreitol (DTT), acetone, acetonitrile, ethylene glycol, iso-propanol, ethylenediaminetetra acetic acid (EDTA), urea, sodium dodecyl sulfate (SDS), phenylmethylsulfonyl fluoride (PMSF), Cetrimonium bromide (CTAB), dimethyl sulfoxide (DMSO), Triton X-100, Tween 20, 3,5-dinitrosalicylic acid (DNS), phosphate buffer, bovine serum albumin (BSA) were all Sigma-Aldrich products. For the cloning, expression and purification of the xylanase the *Nde*I and *Sal*I restriction enzymes (Thermo Fisher Scientific), Gel Extraction kit (Thermo scientific, US), Ni-NTA Fast Start Kit (Qiagen, Hilden, Germany) were used.

2.2. In-silico identification, production and purification of recombinant novel xylanase

The hyper thermostable xylanase from camel rumen microbiota was identified by *in-silico* screening (Gharechahi et al., 2015) and by employing our previously developed tool, TAXyl (Thermal activity prediction for Xylanase) (Shahraki et al., 2019). TAXyl computationally predicts the optimum temperature for xylanase enzymes from glycoside hydrolysis families 10 and 11 utilizing a random forest-based machine learning method in three classes: non-thermo-active (below 50 ℃), thermoactive (between 50 ℃ and 75 ℃), and hyper-thermoactive (above 75 ℃). The metagenomic xylanase enzymes, computationally screened by MetaGeneMark software (Zhu et al., 2010) were presented to the TAXyl and one sequences among them was labeled as hyper-thermo-active. Using standalone NCBI BLAST for the most similar sequence based on pairwise blast with appropriate E-Value was determined. The PROSITE (Hulo et al., 2007) prediction revealed that this enzyme was from GH11 family.

The predicted metagenomic xylanases were evaluated by the NCBI Conserved Domain Database (CDD) (Marchler-Bauer et al., 2017). Also, the tertiary structure of the candidate xylanases was predicted by the Phyre2 tools and AlphaFold (Ronneberger et al., 2021). The pLDDT (per residue Local Distance Difference Test) score and the PAE (Predicted Aligned Error) were used for model validation (Ronneberger et al., 2021).

After computational confirmations, the enzyme we later named it PersiXyn10, was selected and further characterized experimentally.

A forward (5′-AATAGGCTAGCATGGTCTGTTTACAAAAATATG-3′) and reverse (5′-TGATAGGTCGACTTACTGAATCTTCAGATAATC-3′) primers and a camel rumen metagenome DNA template to obtain xylanase gene fragments. For polymerase chain reaction (PCR) amplification, *Nhe*I and *Sal*I restriction sites respectively, were used.

After extracting PCR product from agarose gel 1% (w/v) by the gel extraction kit, the purified DNA fragments were cloned into the pET28a vector as previously described (S. Shohreh Ariaeenejad et al., 2019; S. Ariaeenejad et al., 2019). Then, pET28a plasmid was transformed into

E. coli BL-21 (DE3) cells and the resulting recombinant cell were cultivated at LB medium at 37 ℃. After incubation with IPTG, N-terminal Histidine-tagged recombinant enzyme was purified by utilizing Qiagen Ni-NTA Fast Start Kit(Sadeghian Motahar et al., 2021a). The purified PersiXyn10 was approved by sodium dodecyl sulfate-polyacrylamide gel electrophoresis (SDS-PAGE). The nucleotide sequence of PersiXyn10 was registered in the GenBank with the accession number ON109768.

2.3. Determination of xylanase activity, kinetic constants and spectroscopy studies

The activity of PersiXyn10 was determined by quantification of released reducing sugars using 3,5-dinitrosalicylic acid (DNS) method (Miller, 1959). For this purpose, a ratio of 1:1 birchwood xylan 1% was PersiXyn10 were mixed and kept at 90 ℃ for 15 min followed by the addition of DNS reagent. The reduction of yellow-colored DNS to the orange-red-colored was investigated by recording the absorbance at 540 nm. One unit of xylanase activity was expressed as the 1 μL reducing sugar generated by the xylanase at 1 min (Shohreh Ariaeenejad et al., 2019; S. Ariaeenejad et al., 2019).

To determine the kinetic parameters, enzyme concentrations ranging from 0 to 15 mg/mL (50 mM phosphate buffer, pH 8.0) were incubated with birchwood xylan substrate. The kinetic parameters including K_m, V_{max}, k_{cat} and k_{cat}/K_m were determined using the Michaelis-Menten equation and the Lineweaver-Burk plot of the enzyme kinetics (Shohreh Ariaeenejad et al., 2020; S. Ariaeenejad et al., 2020).

The UV spectrum of PersiXyn10 (0.4 mg/mL in 10 mM phosphate buffer, pH 8.0) was obtained in the range of 200–700 nm (Shimadzu Model 3100 Double-beam Spectrophotometer). The secondary structure was obtained in the far-UV regions (190–260 nm) by circular dichroism (CD) at 25 ℃. Enzyme concentrations were (0.2 mg/mL in 10 mM phosphate buffer, pH 8.0) at 25 ℃. The JASCO J-715 software was used to predict the secondary structure of the protein according to the statistical method (Manavalan and Johnson Jr, 1987). Thermal denaturation of the PersiXyn10 (0.4 mg/mL in 10 mM phosphate buffer, pH 8.0) was followed by measuring at 280 nm (Cary-100 Bio VARIAN spectrophotometer) (Rezaei-Ghaleh et al., 2008). Temperatures were controlled within ± 0.5 ℃ by Cary temperature controller. Absorbance at 280 nm was obtained in the temperature range 25–85 ℃ with a scan rate of 0.5 ℃/min.

2.4. Optimal activity and stability of pH, temperature and storage

To obtain the optimum temperature of the xylanase, the enzyme activity was determined by assessing the enzyme activity over a range of temperatures extending from 30 to 100 ℃ (10 mM phosphate buffer, pH 8.0) for 15 min

The optimal pH of the enzyme was examined by incubating enzyme and substrate in the buffers of different pH values ranging from 4.0 to 11.0 for 20 min in optimal temperature at 90 ℃. The buffers used were 50 mM citrate buffer (pH 4.0–5.0), phosphate buffer (pH 6.0–8.0) and glycine sodium hydroxide buffer (pH 9.0–11.0) (Ariaeenejad et al., 2022).

The thermostability of the PersiXyn10 was exploited by measuring the enzymatic activity after incubation at 30–100 ℃. For the pH stability analysis, the xylanase activity was assayed over a broad pH range of 4.0–11.0 in an appropriate buffer for 24 h (Sadeghian Motahar et al., 2021b).

The influence of storage on the activity of the PersiXyn10 was evaluated by storing the enzyme at 90 ℃ using Eppendorf SmartBlocks (Thermo Fisher Scientific). The enzymatic activity was estimated at one-day intervals during the 30 days period of incubation and the xylanase activity before incubation was set 100% (Mousavi et al., 2022).

2.5. Influence of metallic ions, inhibitors and different solvents on xylanase activity

The reaction mixture containing PersiXyn10 and various ions including K^+, Ca^{2+}, Mn^{2+}, Mg^{2+}, Cu^{2+}, Fe^{2+}, Li^+ Zn^{2+}, Ni^{2+}, and Al^{3+} in concentration of 50 mM, and SDS, urea, EDTA, DTT, Triton X-100, Tween 20, CTAB, PMSF in the concentration of 50 mM and ethanol, methanol, propanol, acetonitrile, acetone, DMSO, ethyleneglycol and isopropanol with concentration of 50% v/v were preincubated with purified enzyme for 30 min at room temperature. Then the mixtures of enzyme and each chemical were conducted at pH 8.0 and 90 ℃ followed by measuring the residual activities. The activity of PersiXyn10 without any chemical additives was considered as 100% (Mousavi et al., 2022).

2.6. Saccharification of paper pulp by the PersiXyn10

Waste paper cartons were used for bio-bleaching studies (Mhiri et al., 2020). To prepare the waste paper carton, first, it is cut into small pieces and thoroughly washed with distilled water; in the next step, the pieces are dismantled using a mill, and the resulting dough oven is dried at 50 ℃. Next, 5% w/v of dried pulp was treated with PersiXyn10 (7 U/g pulp) in phosphate buffer (50 mM, pH 8.0) and incubated for 192 h at 80 °C. A control without enzyme was also kept in parallel. The total reducing sugars were measured by the DNS method.

The changes in the surface of paper carton before and after enzymatic treatment were observed using electron microscopy (SEM) study (FEI ESEM QUANTA 200, USA). The structural analysis of these substrates was also studied by Fourier transform infrared spectroscopy (FTIR) (Thermo, AVATART, Germany) with resolution 4 cm^{-1} in range of 400–4000 cm^{-1} region.

3. Results and discussion

3.1. In-silico identification, cloning, expression and purification of the xylanase sequence

The most similar predicted xylanase, *Fibrobacter* sp. Gut metagenome (E-value 0.0, Query Cover 99% and Total score 540) to glycoside hydrolase family 11 were determined by stand-alone NCBI BLAST software. The PROSITE prediction revealed that the PersiXyn10 has one domain and two nucleophile and proton donor active sites (Glutamic acid) in positions 141 and 239, which are common in GH 11 family (EC 3.2.1.8). The final xylanase candidate was selected by employing the TAXyl, CDD, and Phyre2 tools, AlphaFold and PersiXyn10 was successfully cloned with appropriate expression and selected for further assessments. Analysis of the predicted enzyme from metagenome versus conserved domains using the PSSM models in the CDD, revealed its high similarity with GH11 superfamily members. By 3D modeling of PersiXyn10 using Phyre2 and AlphaFold, its high structural similarity to known xylanase enzymes with confidence score 100% was confirmed. Fig. 1 illustrates the results of the 3D structure of AlphaFold prediction.

After amplifying the sequence of PersiXyn10 from the metagenomic DNA, it was cloned in pET-28a vector and overexpressed in *E. coli* BL21 (DE3). The Ni-NTA Fast Start Kit was used for purified recombinant enzyme. A single band in the SDS-PAGE gel for Persixyn10, were confirmed by a molecular weight corresponding to the 38 kDa (supplementary information).

3.2. Biochemical properties of the hyperthermostable PersiXyn10

The influence of temperature of xylanase activity was determined under temperature ranging from 30 ℃ to 100 ℃ (Fig. 2A). The PersiXyn10 exhibited a gradual upward trend from 30 ℃ to 90℃ and reached the highest activity at 90 ℃ which considered as its optimal temperature. As temperature enhanced from 90℃ to 100 ℃, the enzymatic activity declined slightly and demonstrated 86.53% residual

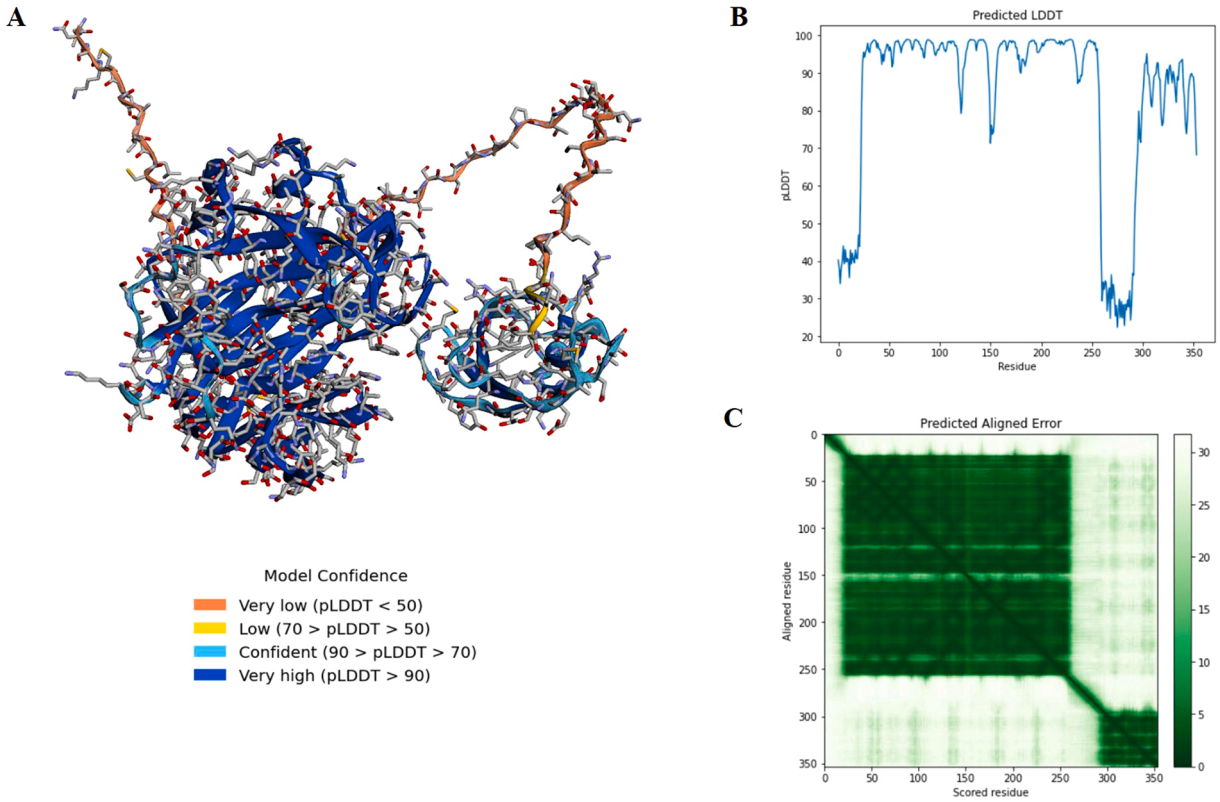

Fig. 1. A) Overview of 3D structure of PersiXyn10 that predicted by Alphafold and pLDDT score for model validation. B) Predicted local distance difference test on each residue. Note that residue from 1 to ~250 are belong to the first domain and ~300–350 are belong to second domain. This plot shows the high pLDDT scores for predicted residues position. C) This figure shows predicted aligned error (PAE) plot. The heatmap indicates expected distance error in Angstroms and gives the estimate of position error at residue x when the predicted and true structures are aligned on residue y. The values range from 0 to 35 angstroms.

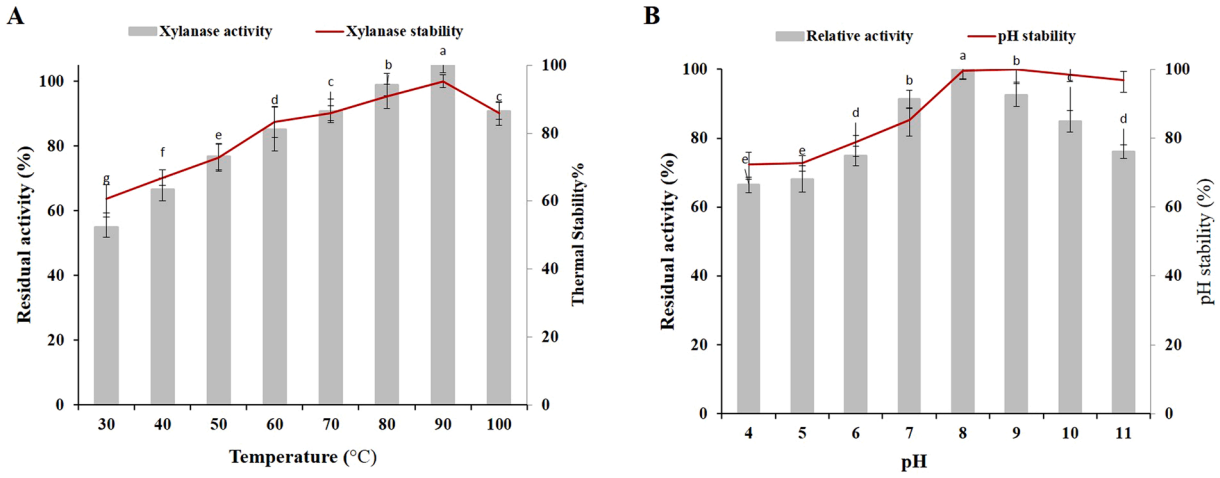

Fig. 2. A) Effect of temperature from 30 to 100℃ and B) pH from 4.0 to 11.0 on the activity of PersiXyn10. Data were analyzed using one-way analyses of variance (ANOVA) on 0.95 level. SPSS software version 22 was used to performed analyses. Three replications were conducted for experiments and means with different letters are significantly different ($p < 0.05$).

activity.

The thermostability analysis showed that the enzyme was stable over wide temperature range 30–100 ℃ (Fig. 2A). the enzyme maintained more than 80% of its activity under temperature 60 ℃ and higher which indicated the xylanase attraction for high temperature industrial applications.

Looking from an overall perception, it is readily apparent that the PersiXyn10 remained more than 60% of its activity under wide range of pH values (Fig. 2B). The maximum enzymatic activity was observed in the pH 8.0 and the xylanase revealed almost equal values at pH 7.0 and 9.0, exhibiting 91.36% and 92.52% activities.

The pH stability studies were accomplished by incubation of the PersiXyn10 pH values from 4.0 to 11.0 for 120 min incubation. According to Fig. 2B, the pH stability profile of the enzyme enhanced remarkably under alkaline conditions and demonstrated that the PersiXyn10 preserved its residual activity over 96% after 24 h incubation under alkaline conditions from pH 8.0–11.0. However, the xylanase was also stable under acidic conditions and presents more than 60% activity

at pH 4.0–6.0 which reached 80% at neutral pH (Fig. 2B).

Some reported xylanase biochemical properties were compared with PersiXyn10 in Table1. The xylanases from metagenome sources as well as other sources are compared with the PersiXyn10 features. The PersiXyn10 demonstrated high thermal stability compared with reported xylanases. Meanwhile, unlike other mentioned xylanases which mainly lost more than 60% of their activity at temperatures 70 ℃ and higher after 60 min incubation, the PersiXyn10 maintained 100% of its activity at 90℃ after 120 min incubation. Additionally, this amount dropped slightly under 100 ℃ indicating the hyper thermostability feature of the enzyme.

In addition, pH stability is another factor that is crucial in increasing the industrial value of xylanases. Based on the results from the pH stability profile of the hyperthermostable alkaline PersiXyn10, its activities were comparably higher than most of the alkaline xylanases (Table1). After 24 h incubation under alkaline conditions, most of the xylanases were inactivated or lost more than 80% of their activities, whereas the PersiXyn10 displayed more than 96% activity at pH 8.0–11.0 which is a favorable characteristic for the enzyme application. To date, hyperthermostable xylanases are effectively used for biorefining purposes due to their high specific activity and good catalytic efficiency at high temperatures. Although different methods have been adopted to improve the thermostability of xylanases(Shohreh Ariaeenejad et al., 2020; S. Ariaeenejad et al., 2020; Norouzi et al., 2020), the *in-silico* screening strategy exhibited high power(Foroozandeh Shahraki et al., 2020; Shahraki et al., 2019). As is observed in Table1, the xylanases identified from various metagenomic sources such as rumen and soil and could withstand extreme pH and temperature which make them highly desirable. This phenomenon confirmed the potential of the metagenomic approach for the discovery of xylanases which are adapted to a wide range of pH and temperature making them promising candidates for extremophilic bioprocessing. Regarding the high activity of the PersiXyn10 as well as its high stability under a broad range of temperatures and pH, it can be applied for various industrial purposes related to high temperatures and in industries that require extreme pH.

3.3. The kinetic parameters of the PersiXyn10

The kinetic values of the PersiXyn10 towards birchwood xylan were evaluated. Based on the outcomes, the K_m, and V_{max} of the PersiXyn10 was found to be 2.65 mg/mL, and 365.19 μmol.mg^{-1}.min^{-1}, respectively. The K_m value of the PersiXyn10 was lower than that of xylanases from *Pediococcus acidilactici* and *Pichia stipitis* using birchwood xylan as substrate (Adiguzel et al., 2019; Ding et al., 2018). While K_m is denoted as the affinity between the enzyme and its substrate, the lower value of this characteristic constant of the enzyme reflects the higher binding affinity of the PersiXyn10. Too, the thermostable PersiXyn10 showed higher V_{max} value than the xylanase from *Paenibacillus barengoltaii* (Liu et al., 2018).

3.4. Storage stability, thermal profiles and circular dichroism measurements

The storage stability of PersiXyn10 was investigated at 90 ℃ for 30 days. As shown in Fig. 3A, the enzyme maintained more than 80% of its activity after being stored for 30 days. Thus, the enzyme was high stable at long-term storage and it shows new feature for using PersiXyn10 in many industrial purposes.

Two known methods for assessing protein stability are protein thermal unfolding and protein-surfactant interactions. The denaturation

Table1
Property comparison of the PersiXyn10 with some known thermostable xylanases.

Source	Optimum temperature (℃)/ pH	Thermostability	pH stability at alkaline condition	Ref
Metagenome-derived	40/8.0	< 20% activity after 60 min incubation at 60 ℃	-	(Shohreh Ariaeenejad et al., 2019; S. Ariaeenejad et al., 2019)
Metagenome-derived	40/9.0	< 80% activity after 120 min incubation at 90 ℃	-	(Shohreh Ariaeenejad et al., 2019; S. Ariaeenejad et al., 2019)
Metagenome-derived	80/9.0	< 40% activity after 120 min incubation at 90 ℃	90% activity after 120 min incubation at pH 11.0	(Verma and Satyanarayana, 2013)
Metagenome-derived	45/6.0	0% activity after 15 min incubation at 70 ℃	< 40% activity after 60 min incubation at pH 11.0	(Al-Darkazali et al., 2017)
Metagenome-derived	40/7.0	< 20% activity after 30 min incubation at 60℃	-	(Hu et al., 2008)
Metagenome-derived	55/6.0	0% activity after 40 min incubation at 60℃	-	(Khalili Ghadikolaei et al., 2017)
Metagenome-derived	35/6.5	0% activity after 60 min incubation at 50℃	90% activity after 24 h incubation at pH 11.0	(Gong et al., 2013)
Metagenome-derived	50/5.0	< 40% activity after 60 min incubation at 70 ℃	< 40% activity after 24 h incubation at pH 11.0	(Kim et al., 2018)
Metagenome-derived	55/7.0	< 40% activity after 60 min incubation at 30 ℃	-	(Qian et al., 2015)
Metagenome-derived	40/7.0	< 20% activity after 15 min incubation at 70 ℃	-	(Jeong et al., 2012)
Aspergillus flavus	55/7.5	0% activity after 30 min incubation at 65 ℃	90% activity after 30 min incubation at pH 10.0	(Chen et al., 2019)
Aspergillus oryzae	30/5.0	< 40% activity after 120 min incubation at 70 ℃	< 80% activity after 30 min incubation at pH 10.0	(Bhardwaj et al., 2020)
Thermoascus aurantiacu	75/5.0	0% activity after 90 min incubation at 90 ℃	< 80% activity after 24 h incubation at pH 10.0	(Ding et al., 2018)
Pediococcus acidilactici	40/7.0	< 20% activity after 120 min incubation at 60 ℃	90% activity after 24 h incubation at pH 9.0	(Adiguzel et al., 2019)
Streptomyces	65/6.5	0% after 60 min at 60 ℃	> 80% after 60 min at pH 10.0	(Li et al., 2009)
Bacillus	65/6.0	0% after 120 min at 75 ℃	80% after 12 h at pH 10.0	(Wang et al., 2019)
Bacillus sp. 30Y5	70/7.0	0% after 20 min at 70 ℃	> 80% after 12 h at pH 10.0	(Li et al., 2021)
Thermobifida halotolerans	70/9.0	0% after 30 min at 80 ℃	< 20% after 150 min at pH 9.0	(Zhang et al., 2012)
Microcella alkaliphila	65/8.0	< 80% after 30 min at 80 ℃	> 80% after 60 min at pH 10.0	(Kuramochi et al., 2016)
Metagenome-derived (PersiXyn10)	90/8.0	100% activity after 120 min incubation at 90℃	96.92% activity after 24 h incubation at pH 11.0	This study

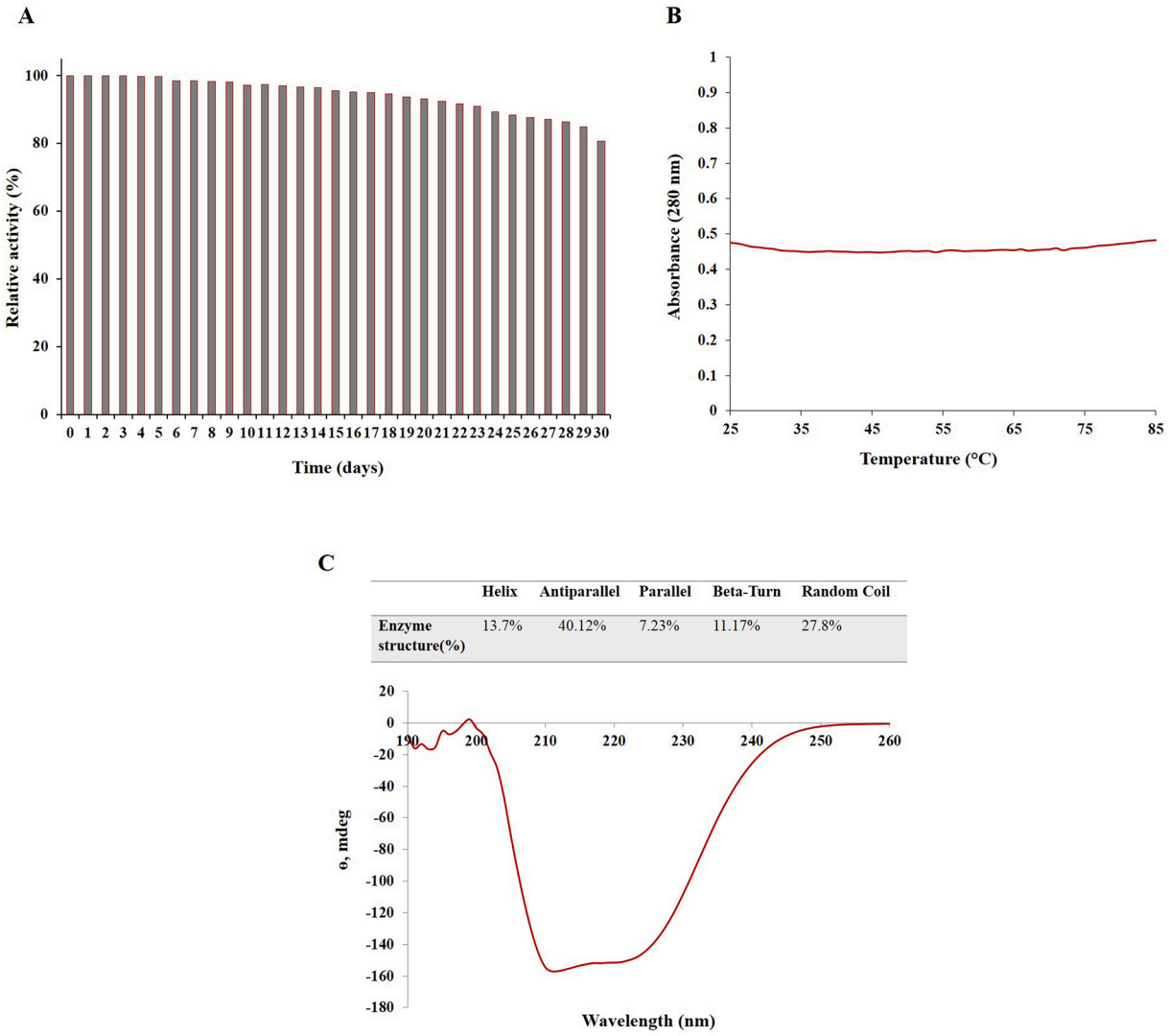

Fig. 3. A) The stability and storage of PersiXyn10 after 30 days incubation at 90 ℃. B) Thermal unfolding curves for PersiXyn10. The enzyme concentration was 0.4 mg/mL dissolved in 10 mM phosphate buffer (pH 8.0), temperature range was 30–85 ℃. The heating rate in experiment was 0.5 ℃/min. C) The far CD spectra was obtained in the range from 190 to 260 nm. The concentration of the enzyme was 0.2 mg/mL dissolved in 10 mM phosphate buffer at pH 8.0, at room temperature. Percentage of different secondary structure of enzyme existed by analyzing the CD spectra.

of the transition between the two macroscopic states of N⇔U from normal (N) to open (U) is defined, and absorption at 280 nm is introduced as a function of temperature for the enzyme (Blanco et al., 2007). By analyzing the thermal unfolding curve of PersiXyn10, expresses that this enzyme does not unfold up to 90 ℃ and hence we could not determine its T_m (Fig. 3B). The percentage of secondary structure elements of PersiXyn10 was helix 13.7%, antiparallel 40.12%, parallel 7.23%, beta-turn 11.17% and 27.8% random coil as measured by CD (Fig. 3C).

Given that it has been suggested that the improved stabilization of the secondary structure involves a higher number of residues in the β-strands, the relatively high percentage of β-sheet elements in the PersiXyn10 structure may partly explain its thermostability properties (Hakulinen et al., 2003).

3.5. Activity of PersiXyn10 in the presence of metal ions, inhibitors and organic solvents

The inhibitory effect of metal ions, inhibitors and organic solvents on the activity of PersiXyn10 was investigated. According to Table2, the xylanase was high resistance to most of the metal ions except Mg^{2+} and Al^{3+}. Meanwhile, the activity of PersiXyn10 was increased after the addition of Mn^{2+}, Ca^{2+}, K^{+}, Fe^{2+}, Cu^{2+}, Li^{2+} and Ni^{2+} and demonstrated various levels of stimulatory effects on the activity of the xylanase. The inhibition or stimulation effects of metal ions on xylanase activity can be due to the interaction of ions with SH or carboxyl groups of enzymes leading to a change in protein conformation and their inactivation (Nagar et al., 2012). It has been reported that xylanases maintained over 80% of their activities in the presence of Mg^{2+} (Basit et al., 2018; Ding et al., 2018). The highest residual activity was observed in the presence of Ca^{2+} and Mn^{+2} which is attributed to the strengthening of interactions inside the protein molecules (Raj et al., 2018). The stimulatory effect of Ca^{2+} and Mn^{+2}on xylanase from *Bacillus amyloliquefaciens* and thermostable xylanase from *Thermotoga naphthophila* were reported (Hamid and Aftab, 2019; Kumar et al., 2017). Additionally, these results were higher than the activity of the metagenome-derived xylanase toward metal ions (Liu et al., 2018).

Besides, the residual activity of the PersiXyn10 in the presence of the various inhibitors was investigated. The addition of urea, PMSF and CTAB declined the xylanase activity. As well, the presence of the EDTA which is a metal chelating compound reduced the enzymatic activity up to 70.31% which indicated the possibility of requirement of some metals

Table2
Influence of metals, chelating and reducing agents and organic solvents, on the activity of the PersiXyn10.

Metal ions	Residual activity (%)
Control	100
Mg^{+2}	81.89
Ca^{+2}	133.05
Mn^{+2}	142.50
Al^{+2}	68.16
Fe^{+2}	129.05
Zn^{+2}	98.74
Cu^{+2}	102.08
Ni^{+2}	111.33
Li^{+2}	109.10
K^{+}	110.01
Inhibitors	Residual activity (%)
SDS	88.39
CTAB	68.75
Tween 20	98.08
Triton X-100	85.95
EDTA	70.31
Urea	53.42
PMSF	64.78
DTT	93.81
Organic solvents	Residual activity (%)
Ethylene glycol	102.08
Ethanol	88.39
Methanol	113.20
Iso-propanol	108.37
Acetonitrile	93.56
DMSO	79.42
Iso-butanol	132.56
Acetone	116.44

for the catalytic activity. These outcomes were in accordance with former studies that introduced a thermo-alkali-stable xylanase from *Aspergillus oryzae* and *Thielaviopsis basicola* (Bhardwaj et al., 2020; Goluguri et al., 2016). In addition, DTT inhibited the enzymatic activity slightly suggesting the distortion of disulfide linkages present between cysteine residues. DTT prevents the forming of disulfide bands by hiding amino acid cysteine of enzyme; therefore, disulfide bonds cannot form internally and externally in the enzyme (Al-Darkazali et al., 2017). Also, different surfactants including Triton-X 100, SDS and Tween 20 could slightly inhibit the activity of the PersiXyn10. SDS can interfere the hydrophobic regions or the structure of a protein causing enzyme denaturation (Bhardwaj et al., 2020).

Further, the enzyme demonstrated high resistance to organic solvents. According to Table2, the addition of the iso-propanol, ethylene glycol, methanol, is-butanol, and acetone motivated the enzymatic activity. By contrast, only slight negative effects were recorded on the PersiXyn10 after the addition of ethanol and acetonitrile. Based on the results, the activity of xylanase decreased when DMSO was added, suggesting that the enzyme deactivation is most probably caused by the disruption of the protein molecule hydrophobic core due to the change of medium hydrophobicity.

3.6. *Biodegradation of paper pulp by the alkaline hyperthermostable PersiXyn10*

Xylanases are an important class of industrial enzymes that are essential for hydrolysis of lignocellulosic biomass into sugars. Particularly, the alkaline and thermostable xylanases are demanded for pulp bleaching in paper and food industry. In the current study the capability of the PersiXyn10 for biodegradation of the pulp paper was studied.

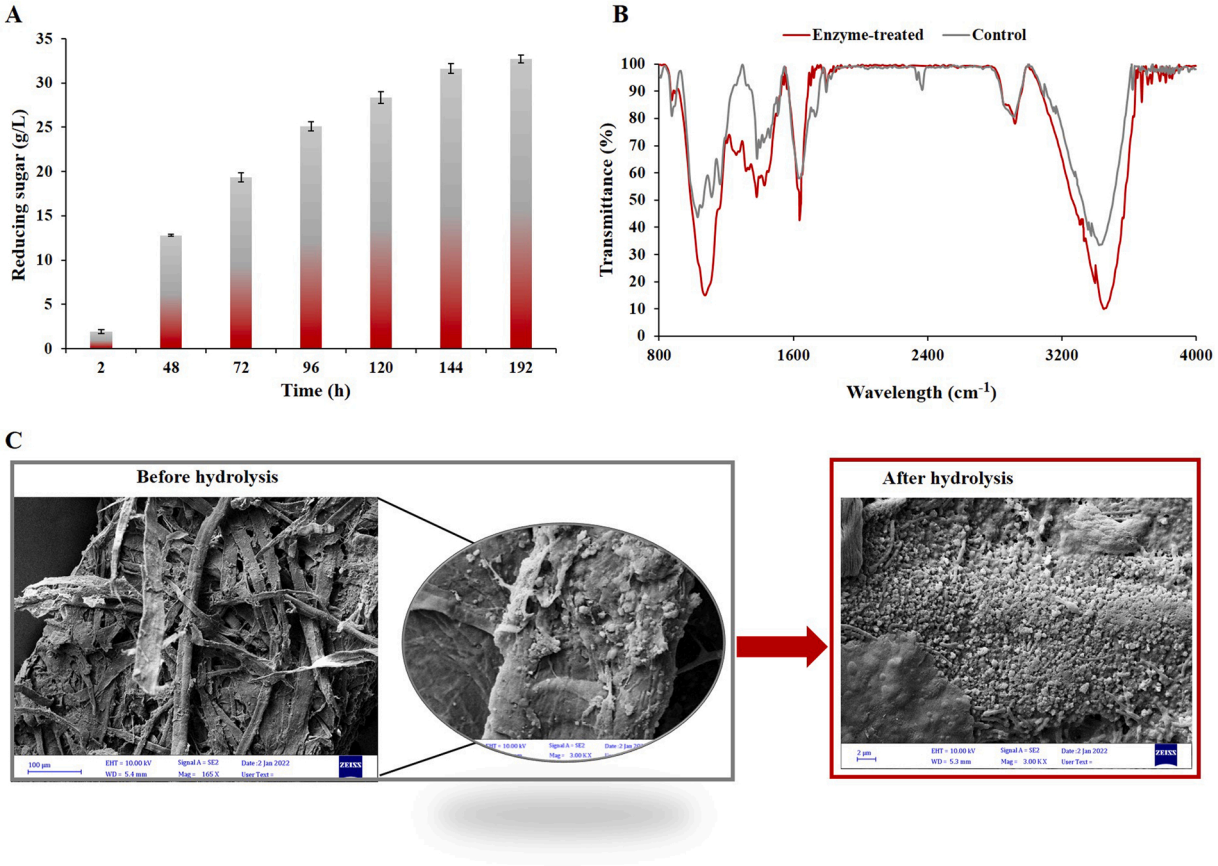

Fig. 4. A) The total reducing sugar produced after the hydrolysis of the pulp paper by the PersiXyn10. B) FTIR spectra of the paper pulp before and after treatment by the PersiXyn10. C) The scanning electron micrograph of paper pulp treated with recombinant enzyme before and after hydrolysis for 192 h under the magnification of 165 KX and 300 KX.

As shown in Fig. 4A, the enzyme reflected the high ability for converting the lignocellulosic to sugars. It was determined that the treatment of the paper pulp with the xylanase enhanced the reducing sugar amount from 1.89 g/L after 2 h to 31.64 g/L after 144 h. These results are in accordance with previous studies which used thermostable xylanase for the modification of pulp paper (Mhiri et al., 2020).

To study the morphological changes of the control and the enzyme treated pulp, the SEM and FTIR analysis was carried out. As stated in the FTIR spectra of the paper pulp before and after treatment by PersiXyn10, various structural changes were carried out during hydrolysis by the xylanase (Fig. 4B). Compared with the control sample, the peak at 3400 cm^{-1} was declined after the xylanase addition. This band is attributed to the OH stretching in cellulose, hemicellulose and lignin (Diaz et al., 2015; Zhuang et al., 2020). The outcomes revealed a reduction at 1639 cm^{-1} in the presence of PersiXyn10 which indicates the aromatic skeletal vibration and C═O stretching of hemicellulose and lignin (Zhuang et al., 2020). Bands at 1165 cm^{-1} and 1029 cm^{-1} are assigned to the symmetric CH_2 bending vibration and symmetric stretching band of carboxyl group in cellulose, hemicellulose and lignin parts of the substrate (Li et al., 2017; Zhuang et al., 2020). Peaks near 1362–1370 cm^{-1} corresponded to cellulose and hemicellulose C-H bending vibration, C-H stretching in CH3 (Gabhane et al., 2020; Zhuang et al., 2020). Also, the band at 1245 cm^{-1} was diminished in the enzyme-treated sample which is attributed to stretching of C-O bands of hemicellulose and lignin (Chen et al., 2016). Bands from 1030 cm^{-1} to 1161 cm^{-1} exhibited C-OH stretching vibration and C-O deformation in cellulose, hemicellulose, lignin and C-O-C asymmetric bridge stretching vibration in cellulose and hemicellulose (Gabhane et al., 2020; Zhuang et al., 2020). These bands decreased remarkably in the xylanase-treated sample confirming the modifications of paper pulp structure by PersiXyn10.

Concerning the SEM micrographs, the samples treated xylanase remarkable changes are observed in the pulp structure compared to the control. The untreated carton pulp was observed development of cracks, pores and peeling (Fig. 4C). The untreated sample presented a compact structure with a smooth surface and no structural deformation. While after enzymatic treatment the original arrangement of the substrate was lost and disrupted into some smaller fragments leading to swelling of pulp (Fig. 4C). Degradation of the paper pulp and the loss of original fiber structure and the development of cracks was reported in former studies during the xylanase treatment (Kumar et al., 2018; Nagar et al., 2013).

These results demonstrated that the PersiXyn10 caused structural changes in the substrate owing to degradation of the fiber present in the paper pulp and release of the reducing sugars. It proved the capability of the novel xylanase to be used in the biobleaching applications.

4. Conclusion

Today, the world is facing the problem of various environmental pollution with the increase in the amount of lignocellulosic waste produced by different industries. Given the concerns about environmental pollution, the presence of microorganisms to overcome this challenge as a producer of robust enzymes is essential for the degradation of this biomass. In this regard, the current study *in-silico* screened the metagenomic data of camel rumen to discover the novel hyperthermostable PersiXyn10. The xylanase was stable at a wide range of temperature and pH and demonstrated worthwhile pH stability by retaining over 95% activity in pH 8.0–9.0 after the incubating for 24 h. The thermostability studies depicted a considerable heat tolerance at elevated temperatures, displaying 80% residual activity after 30 days of storage at 90 ℃, and confirmed the enzyme has strong thermostable properties by biophysical experiments. To investigate the efficiency of the PersiXyn10 as a biobleaching agent, it was subjected to hydrolysis of the paper pulp. The morphological analysis of the paper pulp and the generation of reducing sugars confirmed the modification of the biomass by the xylanase. These results revealed the stable feature of the recombinant enzyme, making it useful for lignocellulosic-based applications.

Ethics statements

NA.

Studies involving animal subjects

No animal studies are presented in this manuscript.

Studies involving human subjects

No human studies are presented in this manuscript.

Inclusion of identifiable human data

No potentially identifiable human images or data is presented in this study.

CRediT authorship contribution statement

Shohreh Ariaeenejad: Conceptualization, Methodology, Writing - original draft, Resources. **Kaveh Kavousi:** Contribute to the computational and bioinformatics data analysis, Writing - review & editing. **Behrouz Zolfaghari**, **Swapnoneel Roy**, **Takeshi Koshiba:** Contributed to the computational data analysis and editing the manuscript. **Ghasem Hosseini Salekdeh**: Supervision, Project administration, Writing - review & editing.

Declaration of Competing Interest

The authors declare that they have no known competing financial interests or personal relationships that could have appeared to influence the work reported in this paper.

Data availability

All data is available in a supplementary file.

Acknowledgements

This work was performed with the assistance of the “Systems and Synthetic Biology department, Agricultural Biotechnology Research Institute of Iran (ABRII)”, and supported in part by "Fidelity National Financial Distinguished Professorship in CIS, 0583–5504-51.".

Appendix A. Supporting information

Supplementary data associated with this article can be found in the online version at doi:10.1016/j.ecoenv.2023.114587.

References

Adiguzel, G., Faiz, O., Sisecioglu, M., Sari, B., Baltaci, O., Akbulut, S., Genc, B., Adiguzel, A., 2019. A novel endo-β-1,4-xylanase from Pediococcus acidilactici GC25; purification, characterization and application in clarification of fruit juices. Int. J. Biol. Macromol. 129. https://doi.org/10.1016/j.ijbiomac.2019.02.054.

Ahmad, T., Singh, R.S., Gupta, G., Sharma, A., Kaur, B., 2019. Metagenomics in the search for industrial enzymes, Biomass, Biofuels. Biochem.: Adv. Enzym. Technol. https://doi.org/10.1016/B978-0-444-64114-4.00015-7.

Al-Darkazali, H., Meevootisom, V., Isarangkul, D., Wiyakrutta, S., 2017. Gene expression and molecular characterization of a xylanase from chicken cecum metagenome. Int. J. Microbiol 2017. https://doi.org/10.1155/2017/4018398.

Ariaeenejad, S., Maleki, M., Hosseini, E., Kavousi, K., Moosavi-Movahedi, A.A., Salekdeh, G.H., 2019. Mining of camel rumen metagenome to identify novel alkali-thermostable xylanase capable of enhancing the recalcitrant lignocellulosic biomass conversion. Bioresour. Technol. 281. https://doi.org/10.1016/j.biortech.2019.02.059.

Ariaeenejad, S., Lanjanian, H., Motamedi, E., Kavousi, K., Moosavi-Movahedi, A.A., Hosseini Salekdeh, G., 2020. The stabilizing mechanism of immobilized metagenomic xylanases on bio-based hydrogels to improve utilization performance: computational and functional perspectives. Bioconjugate Chem. 31. https://doi.org/10.1021/acs.bioconjchem.0c00361.

Ariaeenejad, S., Kavousi, K., Mamaghani, A.S.A., Motahar, S.F.S., Nedaei, H., Salekdeh, G.H., 2021. In-silico discovery of bifunctional enzymes with enhanced lignocellulose hydrolysis from microbiota big data. Int. J. Biol. Macromol. 177, 211–220. https://doi.org/10.1016/j.ijbiomac.2021.02.014.

Ariaeenejad, S., Kavousi, K., Mamaghani, A.S.A., Ghasemitabesh, R., Hosseini Salekdeh, G., 2022. Simultaneous hydrolysis of various protein-rich industrial wastes by a naturally evolved protease from tannery wastewater microbiota. Sci. Total Environ. 815, 152796 https://doi.org/10.1016/J.SCITOTENV.2021.152796.

Ariaeenejad, Shohreh, Hosseini, E., Maleki, M., Kavousi, K., Moosavi-Movahedi, A.A., Salekdeh, G.H., 2019. Identification and characterization of a novel thermostable xylanase from camel rumen metagenome. Int. J. Biol. Macromol. https://doi.org/10.1016/j.ijbiomac.2018.12.041.

Ariaeenejad, Shohreh, Sheykh, A., Mamaghani, A., Maleki, M., Kavousi, K., Shahraki, M. F., Salekdeh, G.H., 2020. A novel high performance in-silico screened metagenome-derived alkali- thermostable endo- β -1, 4-glucanase for lignocellulosic biomass hydrolysis in the harsh conditions. BMC Biotechnol. 20, 1–13.

Atomi, H., Sato, T., Kanai, T., 2011. Application of hyperthermophiles and their enzymes. Curr. Opin. Biotechnol. https://doi.org/10.1016/j.copbio.2011.06.010.

Basit, A., Liu, J., Miao, T., Zheng, F., Rahim, K., Lou, H., Jiang, W., 2018. Characterization of two endo-β-1, 4-xylanases from Myceliophthora thermophila and their saccharification efficiencies, synergistic with commercial cellulase. Front. Microbiol. 9, 1–11. https://doi.org/10.3389/fmicb.2018.00233.

Bhardwaj, N., Verma, V.K., Chaturvedi, V., Verma, P., 2020. Cloning, expression and characterization of a thermo-alkali-stable xylanase from Aspergillus oryzae LC1 in Escherichia coli BL21(DE3). Protein Expr. Purif. 168. https://doi.org/10.1016/j.pep.2019.105551.

Bilal, M., Adeel, M., Rasheed, T., Zhao, Y., Iqbal, H.M.N., 2019. Emerging contaminants of high concern and their enzyme-assisted biodegradation – A review. Environ. Int. https://doi.org/10.1016/j.envint.2019.01.011.

Blanco, E., Ruso, J.M., Sabin, J., Prieto, G., Sarmiento, F., 2007. Thermal stability of lysozyme and myoglobin in the presence of anionic surfactants. J. Therm. Anal. Calor. 87, 211–215.

Chen, L., Li, J., Lu, M., Guo, X., Zhang, H., Han, L., 2016. Integrated chemical and multi-scale structural analyses for the processes of acid pretreatment and enzymatic hydrolysis of corn stover. Carbohydr. Polym. 141, 1–9. https://doi.org/10.1016/j.carbpol.2015.12.079.

Collins, T., Gerday, C., Feller, G., 2005. Xylanases, xylanase families and extremophilic xylanases. FEMS Microbiol. Rev. 29, 3–23.

Diaz, A.B., Moretti, M.M., de, S., Bezerra-Bussoli, C., Carreira Nunes, C., da, C., Blandino, A., da Silva, R., Gomes, E., 2015. Evaluation of microwave-assisted pretreatment of lignocellulosic biomass immersed in alkaline glycerol for fermentable sugars production. Bioresour. Technol. 185, 316–323. https://doi.org/10.1016/j.biortech.2015.02.112.

Ding, C., Li, M., Hu, Y., 2018. High-activity production of xylanase by Pichia stipitis: purification, characterization, kinetic evaluation and xylooligosaccharides production. International Journal of Biological Macromolecules. Elsevier B.V,. https://doi.org/10.1016/j.ijbiomac.2018.05.128.

Foroozandeh Shahraki, M., Ariaeenejad, S., Fallah Atanaki, F., Zolfaghari, B., Koshiba, T., Kavousi, K., Salekdeh, G.H., 2020. MCIC: automated identification of cellulases from metagenomic data and characterization based on temperature and pH Dependence. Front. Microbiol. 11, 1–10. https://doi.org/10.3389/fmicb.2020.567863.

Gabhane, J., Kumar, S., Sarma, A.K., 2020. Effect of glycerol thermal and hydrothermal pretreatments on lignin degradation and enzymatic hydrolysis in paddy straw. Renew. Energy 154, 1304–1313. https://doi.org/10.1016/j.renene.2020.03.035.

Gharechahi, J., Zahiri, H.S., Noghabi, K.A., Salekdeh, G.H., 2015. In-depth diversity analysis of the bacterial community resident in the camel rumen. Syst. Appl. Microbiol. 38, 67–76.

Goluguri, B.R., Thulluri, C., Addepally, U., Shetty, P.R., 2016. Novel alkali-thermostable xylanase from Thielaviopsis basicola (MTCC 1467): purification and kinetic characterization. Int. J. Biol. Macromol. 82, 823–829.

Haile, A., Gelebo, G.G., Tesfaye, T., Mengie, W., Mebrate, M.A., Abuhay, A., Limeneh, D. Y., 2021. Pulp and paper mill wastes: utilizations and prospects for high value-added biomaterials. Bioresour. Bioprocess. https://doi.org/10.1186/s40643-021-00385-3.

Hakulinen, N., Turunen, O., Jänis, J., Leisola, M., Rouvinen, J., 2003. Three-dimensional structures of thermophilic β-1,4-xylanases from Chaetomium thermophilum and Nonomuraea flexuosa: comparison of twelve xylanases in relation to their thermal stability. Eur. J. Biochem. https://doi.org/10.1046/j.1432-1033.2003.03496.x.

Hamid, A., Aftab, M.N., 2019. Cloning, purification, and characterization of recombinant thermostable β-Xylanase Tnap_0700 from thermotoga naphthophila. Appl. Biochem. Biotechnol. 189, 1274–1290. https://doi.org/10.1007/s12010-019-03068-0.

Hulo, N., Bairoch, A., Bulliard, V., Cerutti, L., Cuche, B.A., De Castro, E., Lachaize, C., Langendijk-Genevaux, P.S., Sigrist, C.J.A., 2007. The 20 years of PROSITE. Nucleic Acids Res 36, D245–D249.

Joshi, N., Sharma, M., Singh, S.P., 2020. Characterization of a novel xylanase from an extreme temperature hot spring metagenome for xylooligosaccharide production. Appl. Microbiol. Biotechnol. 104, 4889–4901. https://doi.org/10.1007/s00253-020-10562-7.

Kim, H.Bin, Lee, K.T., Kim, M.J., Lee, J.S., Kim, K.S., 2018. Identification and characterization of a novel KG42 xylanase (GH10 family) isolated from the black goat rumen-derived metagenomic library. Carbohydr. Res 469. https://doi.org/10.1016/j.carres.2018.08.010.

Kumar, N.V., Rani, M.E., Gunaseeli, R., Kannan, N.D., 2018. Paper pulp modification and deinking efficiency of cellulase-xylanase complex from Escherichia coli SD5. Int. J. Biol. Macromol. 111, 289–SD295.

Kumar, Sharad, Haq, I., Prakash, J., Kumar, Sudheer, 2017. Purification, characterization and thermostability improvement of xylanase from Bacillus amyloliquefaciens and its application in pre-bleaching of kraft pulp. 3 Biotech 7, 1–12. https://doi.org/10.1007/s13205-017-0615-y.

Li, F., Zhang, P., Zhang, G., Tang, X., Wang, S., Jin, S., 2017. Enhancement of corn stover hydrolysis with rumen fluid pretreatment at different solid contents: effect, structural changes and enzymes participation. Int. Biodeterior. Biodegrad. 119, 405–412. https://doi.org/10.1016/j.ibiod.2016.10.038.

Liu, X., Liu, Y., Jiang, Z., Liu, H., Yang, S., Yan, Q., 2018. Biochemical characterization of a novel xylanase from Paenibacillus barengoltzii and its application in xylooligosaccharides production from corncobs. Food Chem. 264. https://doi.org/10.1016/j.foodchem.2018.05.023.

Manavalan, P., Johnson Jr, W.C., 1987. Variable selection method improves the prediction of protein secondary structure from circular dichroism spectra. Anal. Biochem. 167, 76–85.

Marchler-Bauer, A., Bo, Y., Han, L., He, J., Lanczycki, C.J., Lu, S., Chitsaz, F., Derbyshire, M.K., Geer, R.C., Gonzales, N.R., Gwadz, M., Hurwitz, D.I., Lu, F., Marchler, G.H., Song, J.S., Thanki, N., Wang, Z., Yamashita, R.A., Zhang, D., Zheng, C., Geer, L.Y., Bryant, S.H., 2017. CDD/SPARCLE: Functional classification of proteins via subfamily domain architectures. Nucleic Acids Res. https://doi.org/10.1093/nar/gkw1129.

Mhiri, S., Bouanane-Darenfed, A., Jemli, S., Neifar, S., Ameri, R., Mezghani, M., Bouacem, K., Jaouadi, B., Bejar, S., 2020. A thermophilic and thermostable xylanase from Caldicoprobacter algeriensis: recombinant expression, characterization and application in paper biobleaching. Int. J. Biol. Macromol. 164. https://doi.org/10.1016/j.ijbiomac.2020.07.162.

Miller, G.L., 1959. Use of dinitrosalicylic acid reagent for determination of reducing sugar. Anal. Chem. 31, 426–428.

Motamedi, E., Kavousi, K., Fatemeh, S., Motahar, S., 2021. Efficient removal of various textile dyes from wastewater by novel thermo-halotolerant laccase. Bioresour. Technol. 337, 125468 https://doi.org/10.1016/j.biortech.2021.125468.

Mousavi, S.H., Sadeghian Motahar, S.S., Salami, M., Kavousi, K., Sheykh Abdollahzadeh Mamaghani, A., Ariaeenejad, S., Salekdeh, G.H., 2022. Invitro bioprocessing of corn as poultry feed additive by the influence of carbohydrate hydrolyzing metagenome derived enzyme cocktail. Sci. Rep. 12, 1–14. https://doi.org/10.1038/s41598-021-04103-z.

Nagar, S., Mittal, A., Gupta, V.K., 2012. Enzymatic clarification of fruit juices (apple, pineapple, and tomato) using purified Bacillus pumilus SV-85S xylanase. Biotechnol. Bioprocess Eng. 17, 1165–1175. https://doi.org/10.1007/s12257-012-0375-9.

Nagar, S., Jain, R.K., Thakur, V.V., Gupta, V.K., 2013. Biobleaching application of cellulase poor and alkali stable xylanase from Bacillus pumilus SV-85S. 3 Biotech. https://doi.org/10.1007/s13205-012-0096-y.

Nigam, P.S., 2013. Microbial Enzymes with Special Characteristics for Biotechnological Applications 597–611. https://doi.org/10.3390/biom3030597.

Norouzi, S., Birgani, N.H., Maghami, P., Ariaeenejad, S., 2020. Improvement of PersiXyn2 activity and stability in presence of Trehalose and proline as a natural osmolyte. Int. J. Biol. Macromol. https://doi.org/10.1016/j.ijbiomac.2020.06.288.

Raj, A., Kumar, S., Singh, S.K., Prakash, J., 2018. Production and purification of xylanase from alkaliphilic Bacillus licheniformis and its pretreatment of eucalyptus kraft pulp. Biocatalysis and Agricultural Biotechnology. Elsevier Ltd. https://doi.org/10.1016/j.bcab.2018.06.018.

Rezaei-Ghaleh, N., Ramshini, H., Ebrahim-Habibi, A., Moosavi-Movahedi, A.A., Nemat-Gorgani, M., 2008. Thermal aggregation of α-chymotrypsin: role of hydrophobic and electrostatic interactions. Biophys. Chem. 132, 23–32.

Ronneberger, O., Tunyasuvunakool, K., Bates, R., Žídek, A., Ballard, A.J., Cowie, A., Romera-paredes, B., Nikolov, S., Jain, R., Adler, J., Back, T., Petersen, S., Reiman, D., Clancy, E., Zielinski, M., Steinegger, M., Pacholska, M., Berghammer, T., Bodenstein, S., Silver, D., Vinyals, O., Senior, A.W., Kavukcuoglu, K., 2021. Highly accurate protein structure prediction with AlphaFold. Nature 596. https://doi.org/10.1038/s41586-021-03819-2.

Sadeghian Motahar, S.F., Ariaeenejad, S., Salami, M., Emam-Djomeh, Z., Sheykh Abdollahzadeh Mamaghani, A., 2021a. Improving the quality of gluten-free bread by a novel acidic thermostable α-amylase from metagenomics data. Food Chem. 352, 129307 https://doi.org/10.1016/j.foodchem.2021.129307.

Sadeghian Motahar, S.F., Salami, M., Ariaeenejad, S., Emam-Djomeh, Z., Sheykh Abdollahzadeh Mamaghani, A., Kavousi, K., Moghadam, M., Hosseini Salekdeh, G., 2021b. Synergistic effect of metagenome-derived starch-degrading enzymes on quality of functional bread with antioxidant activity. Starch/Staerke 2100098, 1–14. https://doi.org/10.1002/star.202100098.

Samsudin, A.A., Wright, A.-D.G., Al Jassim, R., 2012. Investigation into the Cellulolytic Bacteria in the Foregut of the Dromedary Camel (Camelus dromedarius). Appl. Environ. Microbiol. AEM, 02420-12.

Shahraki, M.F., Farhadyar, K., Kavousi, K., Azarabad, M.H., Boroomand, A., Ariaeenejad, S., Salekdeh, G.H., 2019. A generalized machine-learning aided method for targeted identification of industrial enzymes from metagenome: a xylanase temperature dependence case study 1–20. https://doi.org/10.1101/826040.

Tsang, Y.F., Kumar, V., Samadar, P., Yang, Y., Lee, J., Ok, Y.S., Song, H., Kim, K.H., Kwon, E.E., Jeon, Y.J., 2019. Production of bioplastic through food waste valorization. Environ. Int. https://doi.org/10.1016/j.envint.2019.03.076.

Tyagi, D., Sharma, D., 2021. Production and Industrial Applications of Xylanase: A Review 7.

Wang, X., Huang, H., Xie, X., Ma, R., Bai, Y., Zheng, F., You, S., Zhang, B., Xie, H., Yao, B., Luo, H., 2016. Improvement of the catalytic performance of a hyperthermostable GH10 xylanase from Talaromyces leycettanus JCM12802. Bioresour. Technol. 222. https://doi.org/10.1016/j.biortech.2016.10.003.

Yeoman, C.J., Han, Y., Dodd, D., Schroeder, C.M., Mackie, R.I., Cann, I.K.O., 2010. Thermostable Enzymes as Biocatalysts in the Biofuel Industry. Adv. Appl. Microbiol. https://doi.org/10.1016/S0065-2164(10)70001-0.

You, S., Chen, C.C., Tu, T., Wang, X., Ma, R., Cai, H.Y., Guo, R.T., Luo, H.Y., Yao, B., 2018. Insight into the functional roles of Glu175 in the hyperthermostable xylanase XYL10C-ΔN through structural analysis and site-saturation mutagenesis. Biotechnol. Biofuels 11. https://doi.org/10.1186/s13068-018-1150-8.

Zhu, W., Lomsadze, A., Borodovsky, M., 2010. Ab initio gene identification in metagenomic sequences. Nucleic Acids Res 38 e132–e132.

Zhuang, J., Li, M., Pu, Y., Ragauskas, A.J., Yoo, C.G., 2020. Observation of potential contaminants in processed biomass using fourier transform infrared spectroscopy. Appl. Sci. 10, 1–13. https://doi.org/10.3390/app10124345.